

## The non-specificity of dog serum albumin and the *N*-terminal model peptide glycylglycyl-L-tyrosine *N*-methylamide for nickel is due to the lack of histidine in the third position

Jeremy D. GLENNON and Bibudhendra SARKAR

Research Institute, The Hospital for Sick Children, Toronto M5G 1X8, and the Department of Biochemistry, University of Toronto, Toronto M5S 1A8, Ontario, Canada

(Received 22 October 1981/Accepted 8 December 1981)

Equilibrium dialysis of dog serum albumin (DSA) against Ni(II) in 0.1 M *N*-ethylmorpholine/HCl, pH 7.53, demonstrates the absence of a specific Ni(II)-binding site in DSA. To evaluate at the molecular level the influence of the genetic substitution of L-tyrosine for L-histidine at the *N*-terminal of DSA, a simple model tripeptide of the *N*-terminal residues, glycylglycyl-L-tyrosine *N*-methylamide, was synthesized and its Ni(II)-binding properties studied. A comparison of the visible absorption characteristics of Ni(II)-DSA with those of Ni(II)-glycylglycyl-L-tyrosine *N*-methylamide reveals a similar change from octahedral to planar co-ordination as the pH is increased. Both systems exhibit a low Ni(II)-binding affinity at physiological pH, with DSA binding a greater percentage of Ni(II) owing to the availability of at least two binding sites of similar affinities. The complex equilibria between Ni(II) and glycylglycyl-L-tyrosine *N*-methylamide were studied by analytical potentiometry (0.15 M NaCl, 25°C). Four major complex species, MHA, MH<sub>1</sub>A<sub>2</sub>, MH<sub>2</sub>A<sub>2</sub> and MH<sub>3</sub>A [where M and A represent Ni(II) ion and anionic peptide respectively], were detected, MHA being the single species at physiological pH. There is no evidence for the involvement of the phenolic hydroxy group in the octahedral MHA complex, or within the plane of co-ordination in the high-pH species. The results provide direct evidence that the low Ni(II)-binding affinity of DSA is due to the genetic substitution of tyrosine for histidine at the *N*-terminal region of the protein.

Serum albumin is the main transport protein for Ni(II) in human, bovine, rabbit and rat sera (Sunderman, 1977). The mechanism of transportation of Ni(II) in human serum has recently been characterized, as has the nature of the Ni(II)-transport site on HSA (Lucassen & Sarkar, 1979; Laussac & Sarkar, 1980; Glennon & Sarkar, 1982; Sarkar, 1981). The rate of excretion is determined by the distribution of the metal between the low-molecular-weight Ni(II)-binding constituents and the transport protein (Sarkar, 1980). It is in this regard that differences exist in the mode of transportation of Cu(II) and Ni(II) in human serum. Despite this, there are definite similarities in the position and symmetry of binding of both metals. The first four residues in the *N*-terminal amino acid sequence of dog and human albumins (Bradshaw & Peters, 1969; Dixon & Sarkar, 1974) are: Glu-Ala-Tyr-Lys-

and Asp-Ala-His-Lys- respectively. An important role for histidine-3 at the *N*-terminal binding site of HSA has been clearly shown (Iyer *et al.*, 1978; Glennon & Sarkar, 1982). Indeed, in DSA, the absence of a histidine residue in the third position accounts for the lack of specificity for Cu(II) binding (Appleton & Sarkar, 1971; Dixon & Sarkar, 1974). It has been found that the Cu(II) content of dog tissue is uncommonly high and that doses of Cu(II), which do not cause major toxic effects in rats, were lethal to dogs (Goresky *et al.*, 1968). Species differences in the proportions of low-molecular-weight-component-bound and protein-bound Ni(II) stem mainly from variations in the affinities of the albumins for Ni(II) (Callan & Sunderman, 1973). Not unexpectedly, the lack of a histidine residue in the third position has also been alluded to in attempting to explain the reduced affinity of DSA for Ni(II), but conclusive data are lacking.

In the present paper, a detailed examination of the interaction of Ni(II) with DSA by spectrophoto-

Abbreviations used: DSA, dog serum albumin; HSA, human serum albumin.

metry and equilibrium dialysis is reported. To evaluate at the molecular level the influence of the substitution at the *N*-terminal, a simple model of the native-sequence tripeptide glycylglycyl-L-tyrosine *N*-methylamide was synthesized and its Ni(II)-binding properties studied by analytical potentiometry and spectrophotometry.

## Experimental procedures

### Materials

DSA (fraction V, powder) was obtained from the Sigma Chemical Co. (St. Louis, MO, U.S.A.). Subsequent purification by charcoal treatment (Chen, 1967) and gel filtration, followed by treatment with Chelex-100 and dialysis, yielded trace metal-free monomeric protein samples (Sarkar & Wigfield, 1968). The molecular weight was taken to be 69000.  $^{63}\text{NiCl}_2$  (sp. radioactivity 1–10 mCi/mg) was obtained from the Amersham Corporation (Oakville, Ontario). Dialysis membrane was obtained from Visking Co. (c/o Union Carbide, Toronto, Ontario). Benzoxycarbonylglycylglycine was obtained from the Nutritional Biochemicals Corporation (Cleveland, OH, U.S.A.) and L-tyrosine methyl ester hydrochloride from the Sigma Chemical Co. (St. Louis, MO, U.S.A.).

### Synthesis of glycylglycyl-L-tyrosine *N*-methylamide

Benzoxycarbonylglycylglycyl-L-tyrosine methyl ester was synthesized by the mixed anhydride method previously reported for the ethyl ester (Yamashita, 1960). The product was recrystallized from ethyl acetate/diethyl ether (yield 70%; m.p. 168–171°C) and was homogeneous on t.l.c. in the solvent system chloroform/methanol/acetic acid (17:2:1, by vol.) (Kopple *et al.*, 1969). A solution of benzoxycarbonylglycylglycyl-L-tyrosine methyl ester (6.0 g) in methanol (300 ml), cooled in an ice bath, was saturated with methylamine. After 3 h, t.l.c. of the reaction mixture in butan-1-ol/acetone/water/acetic acid (4:3:2:1, by vol.) showed the reaction to be complete. Solvent removal *in vacuo* gave benzoxycarbonylglycylglycyl-L-tyrosine *N*-methylamide as a white solid. The product was recrystallized from hot methanol/diethyl ether [yield 5.5 g (92%); m.p. 225–226°C]. This amide (4.5 g) was suspended in a mixture of methanol (80 ml) and 2M-HCl (5.4 ml) and stirred. Thereafter, 10% Pd on C (450 mg) suspended in water (15 ml) was added into it and the mixture was hydrogenated for 6 h. The catalyst was filtered and the filtrate was evaporated *in vacuo* repeatedly with the addition of methanol. Recrystallization was carried out from hot methanol/ethyl acetate [yield 3.0 g (85%); m.p. 237–238°C]. Amino acid analysis gave Gly/Tyr as 2:1 (Found: C, 49.92; H, 6.08; Cl, 10.29; N, 15.92.

Calc. for  $\text{C}_{14}\text{H}_{21}\text{ClN}_4\text{O}_4$ : C, 48.77; H, 6.1; Cl, 10.3; N, 16.26%.

### Potentiometric titrations

Titrations were performed using a Radiometer automatic-titration apparatus at 25°C, as previously described (Glennon & Sarkar, 1982). Stock solutions were prepared from distilled and deionized water and stored over prepurified argon. Prepurified argon was used to maintain an  $\text{O}_2$ -free atmosphere throughout the titrations. The base used was carbonate-free 0.0980M-NaOH, standardized against weighted amounts of dried potassium hydrogen phthalate. AnalaR  $\text{NiCl}_2 \cdot 6\text{H}_2\text{O}$  was used to prepare a stock 0.1097M- $\text{NiCl}_2$  solution and a direct titration for the determination of the Ni(II) content was carried out by compleximetric titration using Murexide as indicator. Both the proton-ligand and metal-ligand formation constants were determined. In the former case, the titration curves were obtained for three different concentrations of glycylglycyl-L-tyrosine *N*-methyl amide, 0.2 mM, 0.5 mM and 0.8 mM in 0.15M-NaCl and 2.0mM-HCl. For the determination of the metal-ligand stability constants, the initial concentration of HCl was again kept constant and two sets of curves were obtained. The first set was at constant peptide concentration ( $C_A = 0.9253$  mM) with variation of Ni(II) concentration ( $C_M$ ) from zero to 0.1752 mM in steps of 87.6  $\mu\text{M}$ . In the ligand-variation titration curves at constant Ni(II) concentration ( $C_M = 0.1752$  mM), the peptide concentration ( $C_A$ ) varied from 0.9253 mM to 1.619 mM in steps of 0.3469 mM. A very slow reaction was observed in the Ni(II)-peptide titrations in the pH range 7.8–8.8 where a 1 h equilibration period was allowed at each 0.2 pH unit reading.

### Spectrophotometry

Absorbance measurements over the range 340–800 nm were made at 25°C in 1 cm cells with a Beckman Acta MV1 spectrophotometer. For the visible absorption spectra of the 1:1 Ni(II)-DSA complex, solutions were 1.01 mM in 0.15M-NaCl. The reference cell contained DSA of the same concentration. For the Ni(II)-glycylglycyl-L-tyrosine *N*-methylamide system, a similar metal/ligand ratio to those in the titration studies was used. The colour change from blue to yellow coincides with the pH range of slow reaction kinetics, observed in the titration analysis.

### Equilibrium dialysis

An equilibrium dialysis procedure (Lau & Sarkar, 1971) was used to determine the extent of Ni(II) binding to DSA. A typical dialysis unit was formed by fixing together two matched acrylic blocks on either side of a sheet of Visking dialysis tubing, each

block containing a cylindrical chamber of 5 ml capacity with two pieces of perforated Parafilm as lining to seal the compartments. The dialysis buffer was 0.1 M-*N*-ethylmorpholine/HCl, pH 7.53 and  $I = 0.16$ . Each half-unit contained a total of 4 ml of buffer with one half-unit containing a protein concentration of 0.1 mM, in which the Ni(II)/DSA ratio was increased from 0.1 to 3.0. After 6 days of dialysis with gentle shaking at 6°C, equal portions from each pair of compartments were added to 10 ml samples of Aquasol and the samples were counted for  $^{63}\text{Ni(II)}$  radioactivity in a Nuclear-Chicago Mark 1 liquid-scintillation counter.

## Results

### Equilibrium dialysis

The lack of a specific binding site on DSA for Ni(II) is clearly shown for pH 7.53 in Fig. 1, where unbound Ni(II) (mol) per mol of DSA is plotted against an increasing value of the Ni(II)/DSA ratio. The results obtained for HSA are shown for comparison.

### Determination of stability constants

*Proton-glycylglycyl-L-tyrosine N-methylamide (HA) system.* The buffering regions of the amino and phenolic hydroxy groups are partially overlapping. The titration data were processed by the sequential use of three programs (PLOT-3, PKBAR-2 and

LEASK-2), to yield the protonation constants  $\beta_{011}$  and  $\beta_{021}$  of the species HA and  $\text{H}_2\text{A}$  (where A is the anionic form of the peptide) (Lau *et al.*, 1974). The refined  $\text{p}K_a$  values are listed in Table 1.

*Ni(II)-proton-glycylglycyl-L-tyrosine N-methylamide (MHA) system.* The equilibrium occurring between metal ion (M), proton (H) and anionic peptide (A) can be represented by the general reaction equation:



where  $p$ ,  $q$ ,  $r$  are the stoichiometric quantities of M, H and A respectively. The stabilities of the species formed are represented by the stoichiometric equilibrium constant  $\beta_{pqr}$  expressed in terms of concentrations at constant ionic strength, temperature and pressure:

$$\beta_{pqr} = \frac{[M_pH_qA_r]}{m^p h^q a^r}$$

where  $m$ ,  $h$  and  $a$  are the concentrations of free metal ion, hydrogen ion and anionic peptide. The functions to obtain values for the unbound portions of metal ion and ligand A at any specified pH values have been described previously (Sarkar & Kruck, 1973). The experimental data and titration curves [ $-\log h = f(\text{base})$ ] were obtained from the solutions containing different  $C_M$  and  $C_A$ . The data were processed by the PLOT-3 program to give the values for the unbound portions of metal and the proton liberation term  $\delta\text{H}_1^+/\delta C_M$  (Fig. 2), together with  $\delta\text{H}_1^+/\delta C_A$  and the free ligand concentration. Using the data from PLOT-3, the program GUESS-3 set up a matrix of the terms  $m^p h^q a^r$  for each proposed species at each selected pH value. This matrix then served as the input to the program LEASK-4, which uses an iterative least-squares minimization procedure to calculate the stability constants,  $\beta_{pqr}$ . This data processing has been previously reported in detail (Sarkar & Kruck, 1973; Sarkar, 1977a). The proton-liberation data  $\delta\text{H}_1^+/\delta C_M$  when plotted as a function of pH reflects the nature of the complexation reaction. After the onset of complexation at pH 5.4,  $\delta\text{H}_1^+/\delta C_M$  increases very little up to

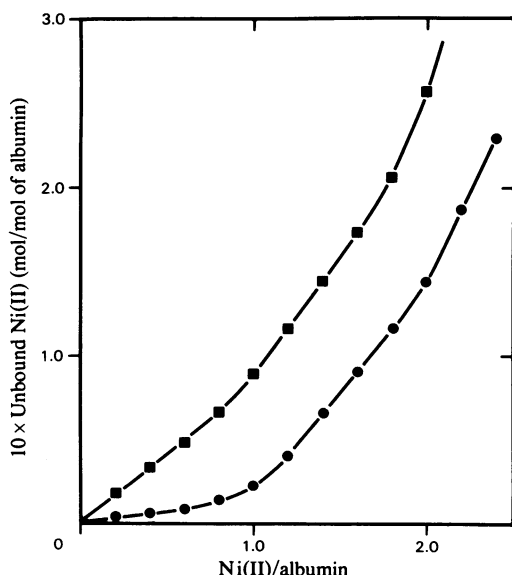


Fig. 1. Equilibrium dialysis at pH 7.53 of DSA (■) and HSA (●) against increasing molar equivalents of Ni(II). The protein concentration is 0.1 mM in 0.1 M-*N*-ethylmorpholine/HCl/0.06 M-NaCl.

Table 1.  $\text{p}K_a$  and  $\log$  stability constants ( $\log \beta_{pqr}$ ) of complex species  $M_pH_qA_r$ , [ $M = \text{Ni(II)}$ ,  $A = \text{glycylglycyl-L-tyrosine N-methylamide}$ ] in 0.15 M-NaCl at 25°C

$p$	$q$	$r$	$\text{p}K_a$	$\log \beta_{pqr}$
0	1	1	9.85	
0	2	1	7.94	
1	1	1		13.28
1	-3	1		-20.69
1	-1	2		2.00
1	-2	2		-7.85

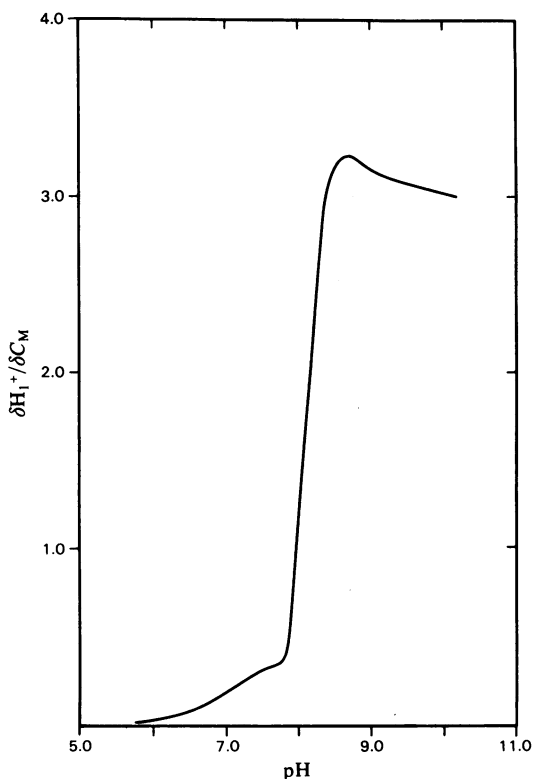


Fig. 2. Molar proton liberation,  $\delta H_1^+ / \delta C_M$  as a function of pH for the Ni(II)-glycylglycyl-L-tyrosine N-methylamide system

pH 7.8. Considerable proton liberation then takes place over a narrow pH range, to a maximum at pH 8.7. At higher pH, there is a levelling of  $\delta H_1^+ / \delta C_M$  toward a value of 3. The sudden increase in proton liberation manifests itself during titration as a sharp change in slope over this narrow pH range. The full distribution of species is shown in Fig. 3. Unbound Ni(II) exists up to pH 8.8 and only 38% of the total Ni(II) is bound by the peptide at pH 7.5. This region of low Ni(II) affinity coincides with the exclusive formation of a protonated MHA species. Between pH 8.2 and 9.4, the bis-complex  $MH_{-1}A_2$  dominates the distribution, with significant amounts of the species MHA,  $MH_{-2}A_2$  and  $MH_{-3}A$ . At higher pH, the latter complex is the major species present. The stoichiometric equilibrium constants  $\beta_{par}$  for the species are given in Table 1.

#### Absorption spectra of DSA and of glycylglycyl-L-tyrosine N-methylamide in the presence of Ni(II)

The absorption spectra of Ni(II)-DSA are shown as a function of pH in Fig. 4. With increasing pH, the octahedral symmetry of co-ordination about Ni(II) persists, as indicated by the peaks at 395 nm

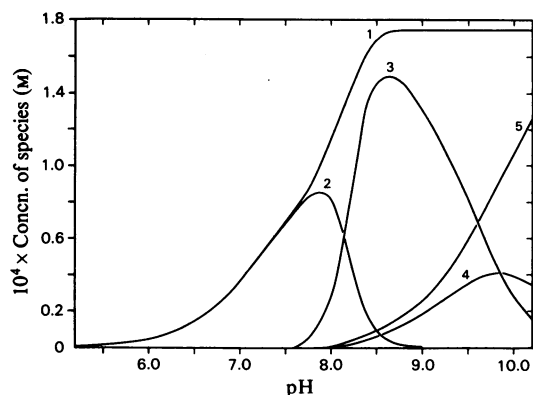


Fig. 3. Species distribution for the Ni(II)-glycylglycyl-L-tyrosine N-methylamide system as a function of pH  $C_M = 0.1752$  mM,  $C_A = 0.9253$  mM; curve 1, bound Ni(II); curve 2, MHA; curve 3,  $MH_{-1}A_2$ ; curve 4,  $MH_{-2}A_2$ ; curve 5,  $MH_{-3}A$ .

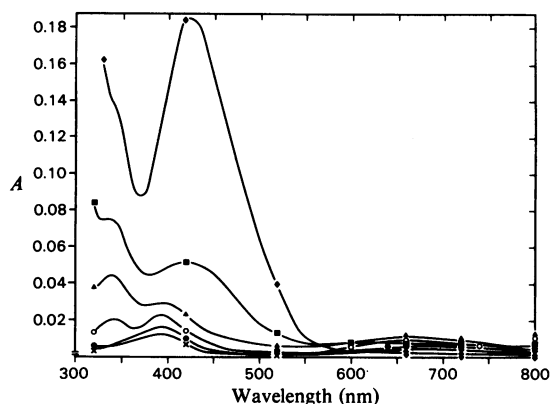


Fig. 4. Visible absorption spectra of DSA in the presence of one equivalent of Ni(II) as a function of pH  $[Ni(II)-DSA] = 1.0$  mM in 0.15 M-NaCl, 1 cm cell pathlength, with protein as reference, at 25°C. x, pH 5.43; ●, pH 6.09; ○, pH 7.31; ▲, pH 8.17; ■, pH 9.05; ◆, pH 10.21.

and 650–720 nm (broad doublet). This is consistent with the absence of a specific binding site for Ni(II). At pH 7.31, some increase in absorption is observed particularly at 340 nm, where a new peak is evident. The binding of Ni(II) would appear to be heterogeneous. The spectra are in sharp contrast with those of Ni(II)-HSA, where the specific binding of the metal manifests itself as a highly absorbing peak at 420 nm characteristic of planar co-ordination at pH 6.9 (Glennon & Sarkar, 1981). Some similarity to the Ni(II)-HSA spectra is achieved as the pH is further increased. A shift toward 420 nm is evident at pH 9.05, whereas by pH 10.21, a planar co-

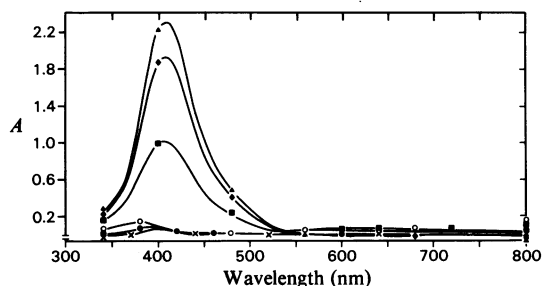


Fig. 5. Visible absorption spectra as a function of pH for the Ni(II)-glycylglycyl-L-tyrosine *N*-methylamide system [Ni(II)] = 10.97 mM; [peptide] = 50.0 mM in 0.15 M-NaCl at 25°C. ×, pH 5.08; ●, pH 5.96. ○, pH 7.31; ■, pH 8.44; ◆, pH 10.06; ▲, pH 11.11.

ordination is indicated by a highly absorbing peak at 425 nm ( $\epsilon_{\max}$ , 184) (Lever, 1968).

A similar change from octahedral to planar symmetry as above is displayed in the Ni(II)-glycylglycyl-L-tyrosine *N*-methylamide system as the pH is increased (Fig. 5). The formation of the MHA species is reflected by the shift of the wavelength maxima from 395 nm and 650–720 nm (doublet) for hexaquo-Ni(II) to 369 nm and 610 (broad peak) as the pH is increased to neutral pH. Although the formation of the planar  $MH_{-1}A_2$  complex exhibits slow reaction kinetics, the change from fully octahedral to fully planar symmetry occurs abruptly over a narrow pH range as shown in these spectra. At pH 8.44, a highly absorbing peak at 407 nm is present. Also present at this pH is a small amount of octahedral Ni(II) as indicated by the presence of a broad peak in the region of 600 nm. Little further change in the wavelength maximum occurs as the pH is raised to 11.11 but there is a noticeable increase in the absorption coefficient as the  $MH_{-3}A$  complex becomes the major species ( $\lambda_{\max}$ , 408,  $\epsilon_{\max}$ , 209).

## Discussion

The contrast between DSA and HSA in the extent of Ni(II) association is evident from the results of the equilibrium dialysis study. The first and second binding sites on DSA display similarly a reduced affinity for Ni(II). A small change in slope is observed after the Ni(II)/DSA ratio reaches 1.0, indicating that a slightly preferred site is present. The subsequent binding sites on both proteins appear to be similar.

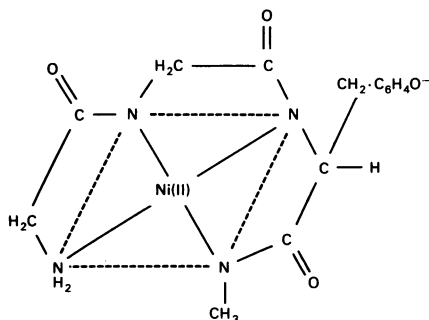
The tripeptide model for *N*-terminal residues of DSA, glycylglycyl-L-tyrosine *N*-methylamide, displays a lack of affinity to bind Ni(II) at physiological pH that actually surpasses that of the protein DSA. This is clearly seen from the species dis-

tribution (Fig. 3), where the concentration of bound Ni(II) is plotted as a function of pH. This is not unexpected, since DSA contains a greater number of possible binding sites. The presence of unbound Ni(II) up to pH 8.8 contrasts with the situation for Ni(II) and the HSA native sequence tripeptide, L-aspartyl-L-alanyl-L-histidine *N*-methylamide, where complete complexation was achieved by pH 7.0 (Glennon & Sarkar, 1982). The present species-distribution analysis together with the spectral data provide direct evidence for the non-interaction of the phenolic hydroxy group of tyrosine with Ni(II) at physiological pH. The u.v. absorption of the tyrosine residue at 274 nm is unaffected by the presence of Ni(II) at pH 7. The shift of the visible absorption maxima of the peaks representing octahedral co-ordination to shorter wavelengths as the pH is increased to 7 is characteristic of nitrogen co-ordination to Ni(II) (Fig. 5) (Cotton & Wilkinson, 1972). Since at this pH the system consists of only the MHA complex, co-ordination involves the amino group of the glycine residue with the phenolic oxygen remaining protonated.

The levelling of the proton liberation  $\delta H_{\dagger}^{\ddagger}/\delta C_M$  at a value of 3 at high pH is very informative. The predominant complex  $MH_{-3}A$  appears to have co-ordination of three peptide nitrogens about Ni(II), similar to the co-ordination of tetraglycine to Ni(II). A plane bordered by the three peptide nitrogens together with the  $\alpha$ -amino nitrogen atom is readily attained. The analogies to the Ni(II)-tetraglycine complex are striking (Martin *et al.*, 1960). There is a co-operative ionization of the peptide hydrogens as planar symmetry is attained, resulting in a pH region of very high buffering capacity. The analysis indicates that the first complex to form on molecular re-arrangement is the bis-complex  $MH_{-1}A_2$ . The maximum wavelength of absorption is constant at 408 nm, as the pH is increased after the appearance of the yellow colour. It is likely that identical groups are involved in the plane of co-ordination in the two species  $MH_{-1}A_2$  and  $MH_{-3}A$ . The proposed pattern of co-ordination is illustrated in Fig. 6 for the  $MH_{-3}A$  complex species. The position of the tyrosine ring with respect to the metal ion is not indicated. Preliminary  $^{13}C$  and  $^1H$  n.m.r. studies on the interaction of Ni(II) with glycylglycyl-L-tyrosine *N*-methylamide in  $^2H_2O$  at high pH have been carried out. Chemical-shift changes for the tyrosine ring resonances and changes in the vicinal coupling constants on complexation indicate a weak aromatic ring interaction with Ni(II) above the plane of co-ordination in the Ni(II) $H_{-3}A$  complex (J. D. Glennon, D. W. Hughes & B. Sarkar, unpublished work). However, aromatic ring interactions with transition metal ions have been suggested for tyrosine-containing tripeptides in the solid and solution state (Franks & Van Der Helm,

Table 2. Visible absorption characteristics and the co-ordinating groups of some planar Ni(II) complexes

Ligand	Groups in the plane of co-ordination			$\lambda_{\max.}$ (nm)	$\epsilon_{\max.}$ (litre·mol <sup>-1</sup> ·cm <sup>-1</sup> )	Reference
	Amino N	Peptide N	Carboxy O			
Gly-Gly-Gly (triglycine)	1	2	1	430	240	Martin <i>et al.</i> (1960)
Gly-L-Leu-L-Tyr	1	2	1	435	225	Koztowski (1978)
Gly-Gly-L-Tyr	1	2	1	430	222	The present work
Gly-Gly-Gly-Gly (tetraglycine)	1	3	0	412	215	Martin <i>et al.</i> (1960)
Gly-Gly-L-Tyr-N-Me	1	3	0	408	209	The present work

Fig. 6. Proposed plane of co-ordination in the  $MH_3A$  complex

1970; Koztowski, 1978). This interaction may be biologically relevant to the oxygenase activity of the copper-containing proteins tyrosinase (Mason, 1966) and caeruloplasmin, where it is speculated that it may facilitate substrate binding to the enzymes.

A compilation of visible-absorption data for various planar Ni(II) complexes within this category is informative (Table 2). Within these complexes, it is clear that the greater the number of peptide nitrogens co-ordinated, the lower is the wavelength of maximum absorption,  $\lambda_{\max.}$ . The similarity of the  $\lambda_{\max.}$  values for Ni(II)-tetraglycine and Ni(II)-glycylglycyl-L-tyrosine *N*-methylamide is a further indication of the non-interaction of the phenolic oxygen within the plane of Ni(II) co-ordination. A comparison of the data for the model peptide glycylglycyl-L-tyrosine *N*-methylamide with that for glycylglycyl-L-tyrosine emphasizes an important criterion in relation to the concept of molecular design to mimic the *N*-terminal metal-binding site of a protein (Sarkar, 1977*b*). The co-ordination tendency of the *C*-terminal carboxy group is evident and should be eliminated by the use of a protecting group. The conversion into the *N*-methylamide is particularly suitable for linear peptides.

The heterogeneity of Cu(II) binding to DSA has been examined (Appleton & Sarkar, 1971); studies

with DSA in the presence of 1 and 2 equiv. of Cu(II) suggest the partitioning of the first equivalent between, at least, two sites. The dialysis profile together with the spectral data strongly indicate that Ni(II) binding is also heterogeneous, particularly at neutral pH. The differences observed in the visible spectra of Ni(II)-DSA and Ni(II)-glycylglycyl-L-tyrosine *N*-methylamide at neutral pH are most likely associated with this heterogeneity of Ni(II) binding to DSA, as opposed to the presence of just a single MHA species in the model peptide system. The model peptide best depicts the mutated 'primary site' of the Ni(II) interaction. At physiological pH, it mimics DSA in its lack of Ni(II)-binding specificity and in the non-involvement of the phenolic hydroxy group of the tyrosine residue in the co-ordination of Ni(II). Thus the lack of a histidine residue in the third position has altered this metal-transport protein to a non-specific Ni(II)-binding protein.

We thank Mrs. J. Breckenridge for her valuable technical assistance. The research was supported by a grant from the Medical Research Council of Canada.

## References

- Appleton, D. W. & Sarkar, B. (1971) *J. Biol. Chem.* **246**, 5040–5046
- Bradshaw, R. A. & Peters, T., Jr. (1969) *J. Biol. Chem.* **244**, 5582–5589
- Callan, W. M. & Sunderman, F. W., Jr. (1973) *Res. Commun. Chem. Pathol. Pharmacol.* **5**, 459–472
- Chen, R. F. (1967) *J. Biol. Chem.* **242**, 173–181
- Cotton, F. A. & Wilkinson, R. G. (1972) in *Advanced Inorganic Chemistry*, 3rd edn., p. 894, J. Wiley and Sons, New York
- Dixon, J. W. & Sarkar, B. (1974) *J. Biol. Chem.* **249**, 5872–5877
- Franks, W. A. & Van Der Helm, D. (1970) *Acta Crystallogr. Sect. B* **27**, 1299–1310
- Glennon, J. D. & Sarkar, B. (1982) *Biochem. J.* **203**, 15–23
- Goresky, C. A., Holmes, T. H. & Sass-Kortsak, A. (1968) *Can. J. Physiol. Pharmacol.* **46**, 771–784
- Iyer, K. S. N., Lau, S., Laurie, S. H. & Sarkar, B. (1978) *Biochem. J.* **169**, 61–69
- Kopple, K. D., Ohnishi, M. & Go, A. (1969) *J. Am. Chem. Soc.* **91**, 4264–4272

- Koztowski, H. (1978) *Inorg. Chim. Acta* **31**, 135–140
- Lau, S. & Sarkar, B. (1971) *J. Biol. Chem.* **246**, 5938–5943
- Lau, S., Kruck, T. P. A. & Sarkar, B. (1974) *J. Biol. Chem.* **249**, 5878–5884
- Laussac, J. -P. & Sarkar, B. (1980) *Can. J. Chem.* **58**, 2055–2060
- Lever, A. B. P. (1968) in *Inorganic Spectroscopy*, Elsevier, Amsterdam
- Lucassen, M. & Sarkar, B. (1979) *J. Toxicol. Environ. Health* **5**, 897–905
- Martin, R. B., Chamberlain, M. & Edsall, J. T. (1960) *J. Am. Chem. Soc.* **82**, 495–498
- Mason, H. (1966) in *The Biochemistry of Copper* (Peisach, J., Aisen, P. & Blumberg, W. E., eds.), p. 340, Academic Press, New York
- Sarkar, B. (1977a) *J. Indian Chem. Soc.* **54**, 117–126
- Sarkar, B. (1977b) in *Metal-ligand Interaction in Organic Chemistry and Biochemistry*, (Pullman, B. & Goldblum N., eds.), pp. 193–228, D. Reidel Publishing Co., Dordrecht
- Sarkar, B. (1980) in *Nickel Toxicology* (Brown, S. S. & Sunderman, F. W., Jr., eds.), pp. 81–84, Academic Press, New York
- Sarkar, B. (1981) in *Coordination Chemistry-21* (Laurent, J. P., ed.), pp. 171–185 I.U.P.A.C./Pergamon Press, Oxford and New York
- Sarkar, B. & Kruck, T. P. A. (1973) *Can. J. Chem.* **51**, 3541–3548
- Sarkar, B. & Wigfield, Y. (1968) *Can. J. Biochem.* **46**, 601–607
- Sunderman, F. W., Jr., (1977) *Ann. Clin. Lab. Sci.* **7**, 377–398
- Yamashita, T. (1960) *J. Biochem. (Tokyo)* **46**, 846–852